

Current Biology

Evolution of the sauropterygian inner ear with increasingly pelagic lifestyles

--Manuscript Draft--

Manuscript Number:	CURRENT-BIOLOGY-D-17-01111R1
Full Title:	Evolution of the sauropterygian inner ear with increasingly pelagic lifestyles
Article Type:	Report
Corresponding Author:	James M Neenan, Ph.D. University of Oxford Oxford, UNITED KINGDOM
First Author:	James M Neenan, Ph.D.
Order of Authors:	James M Neenan, Ph.D. Tobias Reich Serjoscha W Evers Patrick S Druckenmiller Dennis F A E Voeten Jonah N Choiniere Paul M Barrett Stephanie E Pierce Roger B J Benson
Abstract:	<p>Sauroptrygia, a successful clade of marine reptiles abundant in aquatic ecosystems of the Mesozoic, inhabited nearshore to pelagic habitats over >180 million years of evolutionary history [1]. Aquatic vertebrates experience strong buoyancy forces that allow movement in a three-dimensional environment, resulting in structural convergences such as flippers and fish-like bauplans [2, 3], as well as convergences in the sensory systems. We used computed tomographic scans of 19 sauropterygian species to determine how the transition to pelagic lifestyles influenced the evolution of the endosseous labyrinth, which houses the vestibular sensory organ of balance and orientation [4]. Semicircular canal geometries underwent distinct changes during the transition from nearshore Triassic sauropterygians to the later, pelagic plesiosaurs. Triassic sauropterygians have dorsoventrally compact, anteroposteriorly elongate labyrinths, resembling those of crocodylians. In contrast, plesiosaurs have compact, bulbous labyrinths, sharing some features with those of sea turtles. Differences in relative labyrinth size among sauropterygians correspond to locomotory differences: bottom-walking [5, 6] placodonts have proportionally larger labyrinths than actively swimming taxa (i.e. all other sauropterygians). Furthermore, independent evolutionary origins of short-necked, large-headed 'pliosaumorph' body proportions among plesiosaurs coincide with reductions of labyrinth size, paralleling the evolutionary history of cetaceans [7]. Sauroptrygian labyrinth evolution is therefore correlated closely with both locomotory style and body proportions, and these changes are consistent with isolated observations made previously in other marine tetrapods. Our study presents the first virtual reconstructions of plesiosaur endosseous labyrinths and the first large-scale, quantitative study detailing the effects of increasingly aquatic lifestyles on labyrinth morphology among marine reptiles.</p>

Evolution of the sauropterygian inner ear with increasingly pelagic lifestyles

James M. Neenan^{1*}, Tobias Reich², Serjoscha W. Evers³, Patrick S. Druckenmiller⁴, Dennis
F. A. E. Voeten^{5,6}, Jonah N. Choiniere⁷, Paul M. Barrett^{8,7}, Stephanie E. Pierce⁹, Roger B. J.
Benson^{3,7}

¹ Oxford University Museum of Natural History, Parks Road, Oxford, OX1 3PW, UK

² Palaeontological Institute and Museum, University of Zurich, Karl-Schmid-Strasse 4, 8006
Zurich, Switzerland

³ Department of Earth Sciences, University of Oxford, South Parks Road, Oxford, OX1 3AN,
UK

⁴ University of Alaska Museum and Department of Geology and Geophysics, University of
Alaska Fairbanks, 907 Yukon Dr, Fairbanks, AK 99775, USA

⁵ European Synchrotron Radiation Facility, 71 Avenue des Martyrs, 38000, Grenoble, France

⁶ Department of Zoology and Laboratory of Ornithology, Palacký University, 17. listopadu
50, 771 46 Olomouc, Czech Republic

⁷ School of Geosciences and Evolutionary Studies Institute, University of the Witwatersrand,
1 Jan Smuts Ave, Braamfontein 2000, Johannesburg, South Africa

⁸ Department of Earth Sciences, Natural History Museum, Cromwell Road, London SW7
5BD, UK.

⁹ Museum of Comparative Zoology and Department of Organismic and Evolutionary
Biology, Harvard University, Cambridge, Massachusetts, USA

* Corresponding Author and Lead Contact: james.m.neenan@gmail.com

SUMMARY

Sauropterygia, a successful clade of marine reptiles abundant in aquatic ecosystems of the Mesozoic, inhabited nearshore to pelagic habitats over >180 million years of evolutionary history [1]. Aquatic vertebrates experience strong buoyancy forces that allow movement in a three-dimensional environment, resulting in structural convergences such as flippers and fish-like bauplans [2, 3], as well as convergences in the sensory systems. We used computed tomographic scans of 19 sauropterygian species to determine how the transition to pelagic lifestyles influenced the evolution of the endosseous labyrinth, which houses the vestibular sensory organ of balance and orientation [4]. Semicircular canal geometries underwent distinct changes during the transition from nearshore Triassic sauropterygians to the later, pelagic plesiosaurs. Triassic sauropterygians have dorsoventrally compact, anteroposteriorly elongate labyrinths, resembling those of crocodylians. In contrast, plesiosaurs have compact, bulbous labyrinths, sharing some features with those of sea turtles. Differences in relative labyrinth size among sauropterygians correspond to locomotory differences: bottom-walking [5, 6] placodonts have proportionally larger labyrinths than actively swimming taxa (i.e. all other sauropterygians). Furthermore, independent evolutionary origins of short-necked, large-headed ‘pliosaumorph’ body proportions among plesiosaurs coincide with reductions of labyrinth size, paralleling the evolutionary history of cetaceans [7]. Sauropterygian labyrinth evolution is therefore correlated closely with both locomotory style and body proportions, and these changes are consistent with isolated observations made previously in other marine tetrapods. Our study presents the first virtual reconstructions of plesiosaur endosseous labyrinths and the first large-scale, quantitative study detailing the effects of increasingly aquatic lifestyles on labyrinth morphology among marine reptiles.

Key Words: Endosseous labyrinth, semicircular canals, geometric morphometrics, ecomorphology, Mesozoic, palaeoecology

RESULTS

Key ecomorphological hypotheses posit that the geometry of the semicircular canals is fine-tuned to respond to specific sensory inputs imposed by environment, behaviour, and locomotion (e.g. [8-10]). We find that Triassic (nearshore; see Figure S1 for definitions) sauropterygians have labyrinths similar to the generalized reptilian morphology [11] (Figures 1 and 2; Figure S2; Table S1), and are anteroposteriorly long with gracile semicircular canals and a narrow crus communis, the dorsal extent of which is embayed in a distinct ‘M’-shape by the medial portions of the anterior and posterior canals. The anterior canal extends higher dorsally and further anteriorly relative to the posterior canal (and is thus longer in total). The horizontal canal is relatively straight and does not bow out far laterally. The posterior canal is highly sinusoidal (deviating from planarity) in the Triassic *Placodus* and *Nothosaurus*, and is somewhat sinusoidal in *Augustasaurus*.

In contrast, plesiosaurs (Figures 1 and 2; Figures S2 and S3) have a more compact, bulbous labyrinth, with a wider crus communis, semicircular canals that are more elliptical in lateral view, shorter, wider in cross-sectional diameter, and lack sinusoidal curvature. The anterior and posterior vertical canals are subequal in both height and total length, and the horizontal canal bows out laterally. The larger cross-sectional diameters of plesiosaurian semicircular canals could result from increases in the diameters of the endosseous canals due to relaxed ossification (i.e. with no underlying change in the membranous labyrinth). However, other differences between plesiosaur and non-plesiosaur labyrinths cannot be explained this way because they involve changes in the aspect ratios and relative arc lengths of individual canals that could not easily be accommodated by purely increasing the diameters of the endosseous canals.

Principal components analysis of 3D landmarks on the semicircular canals (STAR Methods) show that much of the shape variation in sauropterygian labyrinths is explained by

the differences between the nearshore Triassic sauropterygians and pelagic plesiosaurs described above. Our first principal components axis separates these two groups and explains 37.1% of total shape variance (Figure 2). This shows that the labyrinth changed substantially during the evolution of pelagic lifestyles. PC2 explains 16.8 % of shape variance (Figure 2A), and predominantly describes variation in the aspect ratio of the labyrinth (dorsoventral height:anteroposterior length). The elasmosaurid plesiosaur *Callawayasaurus* has a high negative PC2 score, indicating a proportionally tall labyrinth. This is evident from the portion preserved in UCMP V-38349 (Figure S2H), showing that the PC2 score of *Callawayasaurus* does not result from our use of a composite reconstruction for this taxon. In contrast, our other elasmosaurid, *Libonectes* has a high positive PC2 score and a proportionally low labyrinth. PC3 is the only axis to show statistically significant (phylogenetic regression) or marginally significant (ordinary least squares regression) correlation with labyrinth centroid size, and explains at best a low proportion of variance in PC3 (34%, phylogenetic regression; Table S2), which itself describes only 12.2% of shape variance. This suggests only a limited role for allometry in determining shape variance among the labyrinths of sauropterygians (Table S2). PC3 also describes changes in the geometry of the horizontal canal, with negative values indicating a shorter, more posteriorly positioned horizontal canal, while positive values have a longer horizontal canal with a more anterior projection.

Labyrinth size correlates positively with skull length in Sauropterygia (Figure 3), exhibiting negative allometry with coefficients ranging from 0.46–0.80 across 100 phylogenies among regression models with non-negligible AICc weights (STAR Methods). The best model according to AICc across all phylogenies includes only skull length as an explanation of labyrinth size (Table S3; AICc weight = 0.64). Head size is the most appropriate comparative measure of size, because sensory inputs from the labyrinth are specifically involved in head stabilisation [12, 13]. However, a low R^2 value (= 0.27)

indicates considerable unexplained variance in this model. Two other models have non-negligible AICc weights (at least 10% that of the best model), indicating that they cannot be rejected based on current data. Both models include other variables in addition to skull length, and AICc is a highly conservative test of model support given small sample size [14]. These models include categorical variables to code the presence of swimming (as opposed to bottom walking in placodonts (see STAR Methods); AICc weight = 0.15) or to code the presence of both swimming and pliosauromorph body proportions, comprising a large head and short neck (AICc weight = 0.08) (Table S3).

Our third model (Table S3) explains greater variance than the others ($R^2 = 0.37$), and encapsulates the hypothesis that sauropterygian labyrinth size is determined by skull size, the presence of swimming, and the presence of short necks, for which all coefficients have statistically significant values. These coefficients indicate that bottom-walking placodonts have proportionally larger labyrinths than other, swimming, taxa, and that short-necked plesiosaurs (thalassophonean pliosaurids and polycotylids) have proportionally reduced labyrinth sizes (Figure 3). The relatively weaker AICc weight of this model compared to others encourages caution in making strong, process-based interpretations of its parameters.

DISCUSSION

We find evidence for smaller labyrinth sizes in all predominantly swimming sauropterygians compared to those of placodonts. Among swimmers, ‘pliosauromorph’ plesiosaurs (i.e. those with short necks; [15]), having particularly small labyrinths in proportion to head size (Figure 3). Although labyrinth size did not change during the transition from nearshore sauropterygians, such as placodonts and nothosaurs, to pelagic sauropterygians (i.e. plesiosaurs), large changes in labyrinth shape did occur. The timing of shape changes is therefore decoupled from the occurrence of size changes (Figure 1), and we

suggest that they reflect a response to novel sensory inputs that result from the unique and enigmatic four-flippered underwater flight of plesiosaurs [16-21].

The geometry of the plesiosaur labyrinth is not only distinct from that of Triassic sauropterygians (Figure 1), but also from other nearshore/semi-aquatic marine reptiles, including most extant marine reptiles (Figure 4). Considering the relatively small differences between the labyrinths of extant reptiles and those of Triassic sauropterygians [11], this suggests that adaptation from nearshore/semi-aquatic to pelagic life involved a more radical transformation of the vestibular organ than that involved in adaptation to nearshore or semi-aquatic habitats. Among amniotes, chelonoids (sea turtles) and cetaceans, as well as the extinct thunnosaurian ichthyosaurs (and possibly mosasaurs), also obtained a similar grade of pelagic adaptation to that seen in plesiosaurs [1] (Figure S1). However, of these, little is known of ichthyosaur labyrinth morphology, and the labyrinth of cetaceans is fundamentally different in structure to that of plesiosaurs, resembling those of other mammals (Figure 4), albeit with a highly reduced relative canal size [7, 22, 23]. This, and the observation that penguin labyrinths are most similar to those of other birds [24] (Figure 4G), suggests that ancestry can constrain the geometry of the amniote labyrinth, despite the expectation that similar functional inputs should result from a secondarily aquatic lifestyle.

Nevertheless, within reptiles (other than birds), striking similarities are evident between the geometry of some sauropterygian labyrinths, and those of other groups. Nearshore (Triassic) sauropterygians exhibit long, narrow semicircular canals, a narrow crus communis, a taller anterior canal, and a general rounded or pyramidal shape in lateral view that creates an ‘M’-shaped outline (Figure 1). An extremely similar morphology is present in aquatic and semi-aquatic members of the crocodylian total-group (Pseudosuchia), including phytosaurs [25], thalattosuchians [26, 27] and modern crocodylians such as *Alligator* and *Crocodylus* [24, 27, 28] (Figure 4). Shared features are also present in freshwater aquatic

turtles and marine squamates (Figure 4). These features may be common to shallow-water aquatic reptiles in general [24], most of which rely on lateral undulation of the trunk and tail to generate propulsion under water. The labyrinths of obligate aquatic plesiosaurs depart substantially from this condition, and share many (but not all) features with another group that uses predominantly limb-driven underwater flight in combination with a rigid trunk: sea turtles. Both plesiosaurs and sea turtles exhibit shorter semicircular canals with wider cross-sectional diameters, anterior and posterior canals that are roughly equal in height, and a wide crus communis [29] (Figure 4). Therefore, our observations indicate that convergent evolution of aquatic and subsequently pelagic habits has produced similar labyrinth morphologies in independent evolutionary lineages at least in non-avian reptiles.

Despite conspicuous differences between the labyrinths of reptiles and mammals, some functional signals might still be shared between these phylogenetically distant groups during adaptation to aquatic life. In particular, the anterior semicircular canal of nearshore sauropterygians is always higher/longer than the posterior one, which is similar to the condition generally seen in mammals (including cetaceans, and also terrestrial species), and has been linked to sensitivity to pitch movements [8, 10, 30].

Similar evolutionary patterns of labyrinth size variation are also seen in both plesiosaurs and cetaceans. Plesiosaurs independently evolved large-headed, short-necked, cetacean-like body proportions at least twice during their evolutionary history [15]: in both cases this correlates with proportional miniaturisation of the labyrinth (Figure 3). Extant cetaceans also have these body proportions and have proportionally miniaturised labyrinths [7, 22]. Previously, it was not clear whether labyrinth miniaturisation resulted from adaptation to pelagic life, or from proportional neck reduction. Because pelagic sauropterygians (= plesiosaurs) with elongate or intermediate-length necks do not have miniaturised labyrinths, it seems likely that labyrinth miniaturisation results from neck

reduction in pelagic animals, and not strictly from pelagic adaptation alone. Functional interpretation of this pattern remains challenging. Dramatic shortening of the cervical series may decrease the need for reflex-stabilization of the head with the cervical musculature (vestibulo-colic reflex [31]). It is possible that the reduced arcs of cetacean and short-necked plesiosaur semicircular canals had reduced sensitivities, counteracting the increased levels of uncompensated angular motion due to the lack of neck stabilization [7, 32]. However, Kandel & Hullar [23] found cetacean (the bottlenose dolphin, *Tursiops*) head accelerations are similar to those of terrestrial mammals (*Bos*), challenging the assumption that neck shortening results in changes to habitual head accelerations. It has been proposed in cetaceans that the vestibulo-ocular reflex of the eye muscles, which is mediated by vestibular sensory inputs and informs gaze stabilisation during head movement [31], may have been partially replaced by enhanced sensitivity to the sound of water passing the external ear, or the sensation of water passing over the skin [23, 33]. However, it is difficult for this cetacean-specific hypothesis to also explain the parallel reductions of labyrinth size in short-necked plesiosaurs.

In conclusion, we introduce the first virtual reconstructions of plesiosaur endosseous labyrinths and examine the effects of aquatic specialization on labyrinth geometry in reptiles. We show that early sauropterygians, living in nearshore waters, have a crocodylian-like morphology, including some plesiomorphies that are widely present among reptiles [11]. In contrast, derived, pelagic plesiosaurs, have highly modified labyrinths somewhat similar to those of sea turtles. Independent origins of short-necks and large heads among plesiosaurs resulted in cetacean-like body proportions, and these taxa show convergent evolutionary reductions in labyrinth size, similar to that in cetaceans. Our results show that inner ear morphology can be affected greatly by both swimming mode (bottom-walking/jointed limbs

vs. flippered swimming) and by variation in mechanical inputs due to proportional changes in neck length (pliosauromorph plesiosaurs vs. other plesiosaurs).

AUTHOR CONTRIBUTIONS

JMN, SEP and RBBJ designed the research. JMN and RBBJ carried out the research and wrote the paper. JMN, RBBJ, TR, SWE, PSD, DFAEV, JNC, PMB provided datasets to the study and contributed to manuscript preparation. The authors declare no conflicts of interest.

ACKNOWLEDGMENTS

Our sincere thanks go to the numerous curators, technicians and others who made specimen access and scanning possible: S. Chapman and Richard Abel (NHMUK); T. Davies and B. Moon (U. Bristol); M. Evans (LEICT); D. Gelsthorpe, K. Bates, P. Falkingham, M. Johnson (U. Manchester); H. Ketchum (OUMNH); S. Brandt (discoverer and preparator of NME 16/4); M. Hartmann (NME); V. Fernandez and P. Tafforeau (ESRF); M. Garcia and G. Clement (MNHN); P. Holroyd (UCMP); M. Colbert, W. Gelnaw and J. Maisano (U. Texas); Zhe-Xi Luo and A. Neander (U. Chicago); O. Rieppel, W. Simpson and A. Resatar (FMNH); J. Rabold (UMO); M. Böhme, H. Stöhr, P. Havlik and I. Werneburg (GPIT); A. Kupfer (SMNS); J. Scannella and J. Horner (MOR); R. Smith and Z. Erasmus (SAM). D. Davesne, H. Drage, D. Ford, S. Giles, D. Murdock, I. Rahman, E. Saupe and A. Wolniewicz (U. Oxford), T. Scheyer, G. Aguirre Fernández, A. Latimer, S. Spiekman, T. Argyriou and A. Treindl (Zurich), and M. Friedman (Michigan) are also thanked for useful discussions. We are grateful to the two anonymous reviewers for their helpful comments. This research was primarily funded by a Swiss National Science Foundation (SNSF) Early Postdoc Mobility Grant awarded to JMN (P2ZHP3_162102), with additional research grants from the John Fell Oxford University Press Fund (162/060) and the European Association of Vertebrate

Palaeontologists (EAVP). TR is funded by SNSF grant 31003A_173173, and JNC is funded by the National Research Foundation of South Africa's African Origins Platform and the DST/NRF Centre of Excellence in Palaeosciences grants.

REFERENCES

1. Motani, R. (2009). The evolution of marine reptiles. *Evol. Educ. Outreach* 2, 224–235.
2. Motani, R. (2005). Evolution of fish-shaped reptiles (Reptilia: Ichthyopterygia) in their physical environments and constraints. *Annu. Rev. Earth Planet. Sci.* 33, 395–420.
3. Kelley, N.P., and Pyenson, N.D. (2015). Evolutionary innovation and ecology in marine tetrapods from the Triassic to the Anthropocene. *Science* 348, aaa3716.
4. Sipla, J.S., and Spoor, F. (2008). The physics and physiology of balance. In *Sensory Evolution on the Threshold: Adaptations in Secondarily Aquatic Vertebrates*, J.G.M. Thewissen and S. Nummela, eds. (Berkeley: University of California Press), pp. 227–232.
5. Scheyer, T.M., Neenan, J.M., Renesto, S., Saller, F., Hagdorn, H., Furrer, H., Rieppel, O., and Tintori, A. (2012). Revised paleoecology of placodonts – with a comment on ‘The shallow marine placodont *Cyamodus* of the central European Germanic Basin: its evolution, paleobiogeography and paleoecology’ by C.G. Diedrich (Historical Biology, iFirst article, 2011, 1–19, doi: 10.1080/08912963.2011.575938). *Hist. Biol.* 24, 257–267.
6. Klein, N., Houssaye, A., Neenan, J.M., and Scheyer, T.M. (2015). Long bone histology and microanatomy of Placodontia (Diapsida: Sauropterygia). *Contrib. Zool.* 84, 59–84.

7. Spoor, F., Bajpai, S., Hussain, S.T., Kumar, K., and Thewissen, J.G.M. (2002). Vestibular evidence for the evolution of aquatic behaviour in early cetaceans. *Nature* 417, 163–166.
8. Spoor, F., Garland, T., Krovitz, G., Ryan, T.M., Silcox, M.T., and Walker, A. (2007). The primate semicircular canal system and locomotion. *Proc. Natl. Acad. Sci. U.S.A.* 104, 10808–10812.
9. Malinzak, M.D., Kay, R.F., and Hullar, T.E. (2012). Locomotor head movements and semicircular canal morphology in primates. *Proc. Natl. Acad. Sci. U.S.A.* 109, 17914–17919.
10. Ekdale, E.G. (2016). Form and function of the mammalian inner ear. *J. Anat.* 228, 324–337.
11. Baird, I.L. (1970). The anatomy of the reptilian ear. In *Biology of the Reptilia*. Vol. 2 Morphology B, C. Gans and T.S. Parsons, eds. (London: Academic Press), pp. 193–275.
12. Jones, G.M., and Spells, K.E. (1963). A theoretical and comparative study of the functional dependence of the semicircular canal upon its physical dimensions. *Proc. R. Soc. B* 157, 403–419.
13. Georgi, J.A., Sipla, J.S., and Forster, C.A. (2013). Turning semicircular canal function on its head: dinosaurs and a novel vestibular analysis. *PLOS ONE* 8, e58517.
14. Burnham, K.P., and Anderson, D.R. (2002). Model selection and multimodel inference: a practical information-theoretic approach, 2nd Edition, (New York: Springer-Verlag).
15. O'Keefe, F.R. (2002). The evolution of plesiosaur and pliosaur morphotypes in the Plesiosauria (Reptilia: Sauropterygia). *Paleobiology* 28, 101–112.

16. Storrs, G.W. (1993). Function and phylogeny in sauropterygian (Diapsida) evolution. *Am. J. Sci.* 293, 63–90.
17. Watson, D.M.S. (1924). The elasmosaurid shoulder-girdle and fore-limb. *J. Zool.* 94, 885–917.
18. Robinson, J.A. (1975). The locomotion of plesiosaurs. *Neues Jahrb. Geol. Paläontol.* 149, 286–332.
19. O'Keefe, F.R., and Carrano, M.T. (2005). Correlated trends in the evolution of the plesiosaur locomotor system. *Paleobiology* 31, 656–675.
20. Liu, S., Smith, A.S., Gu, Y., Tan, J., Liu, C.K., and Turk, G. (2015). Computer simulations imply forelimb-dominated underwater flight in plesiosaurs. *PLOS Comput. Biol.* 11, e1004605.
21. Muscutt, L.E., Dyke, G., Weymouth, G.D., Naish, D., Palmer, C., and Ganapathisubramani, B. (2017). The four-flipper swimming method of plesiosaurs enabled efficient and effective locomotion. *Proc. R. Soc. B* 284, 20170951.
22. Spoor, F., and Thewissen, J.G.M. (2008). Comparative and functional anatomy of balance in aquatic mammals. In *Sensory Evolution on the Threshold: Adaptations in Secondarily Aquatic Vertebrates*, J.G.M. Thewissen and S. Nummela, eds. (Berkeley: University of California Press), pp. 257–284.
23. Kandel, B.M., and Hullar, T.E. (2010). The relationship of head movements to semicircular canal size in cetaceans. *J. Exp. Biol.* 213, 1175–1181.
24. Georgi, J.A., and Sipla, J.S. (2008). Comparative and functional anatomy of balance in aquatic reptiles and birds. In *Sensory Evolution on the Threshold. Adaptations in Secondarily Aquatic Vertebrates*, J.G.M. Thewissen and S. Nummela, eds. (Berkeley: University of California Press), pp. 233–256.

25. Lautenschlager, S., and Butler, R.J. (2016). Neural and endocranial anatomy of Triassic phytosaurian reptiles and convergence with fossil and modern crocodylians. *PeerJ* 4, e2251.
26. Pierce, S.E., Williams, M., and Benson, R.B.J. (2017). Virtual reconstruction of the endocranial anatomy of the early Jurassic marine crocodylomorph *Pelagosaurus typus* (Thalattosuchia). *PeerJ* 5, e3225.
27. Brusatte, S.L., Muir, A., Young, M.T., Walsh, S., Steel, L., and Witmer, L.M. (2016). The braincase and neurosensory anatomy of an Early Jurassic marine crocodylomorph: implications for crocodylian sinus evolution and sensory transitions. *Anat. Rec.* 299, 1511–1530.
28. Witmer, L.M., Ridgely, R.C., Dufeu, D.L., and Semones, M.C. (2008). Using CT to peer into the past: 3D visualization of the brain and ear regions of birds, crocodiles, and nonavian dinosaurs. In *Anatomical Imaging. Towards a New Morphology*, H. Endo and R. Frey, eds. (Tokyo: Springer), pp. 67–87.
29. Walsh, S.A., Barrett, P.M., Milner, A.C., Manley, G., and Witmer, L.M. (2009). Inner ear anatomy is a proxy for deducing auditory capability and behaviour in reptiles and birds. *Proc. R. Soc. B* 276, 1355–1360.
30. Ekdale, E.G. (2013). Comparative anatomy of the bony labyrinth (inner ear) of placental mammals. *PLOS ONE* 8, e66624.
31. Land, M.F. (2015). Eye movements of vertebrates and their relation to eye form and function. *J. Comp. Physiol. A* 201, 195–214.
32. Yang, A., and Hullar, T.E. (2007). Relationship of semicircular canal size to vestibular-nerve afferent sensitivity in mammals. *J. Neurophysiol.* 98, 3197–3205.
33. Ridgway, S.H., and Carder, D.A. (1990). Tactile sensitivity, somatosensory responses, skin vibrations, and the skin surface ridges of the bottlenose dolphin,

- Tursiops truncatus*. In *Sensory Abilities of Cetaceans*, J.A. Thomas and R.A. Kastelein, eds. (New York: Plenum Press), pp. 163–179.
34. Tambussi, C.P., Degrange, F.J., and Ksepka, D.T. (2015). Endocranial anatomy of Antarctic Eocene stem penguins: implications for sensory system evolution in Sphenisciformes (Aves). *J. Vert. Paleontol.* 35, e981635.
 35. Yi, H., and Norell, M.A. (2015). The burrowing origin of modern snakes. *Sci. Adv.* 1, e1500743.
 36. Cuthbertson, R.S., Maddin, H.C., Holmes, R.B., and Anderson, J.S. (2015). The braincase and endosseous labyrinth of *Plioplatecarpus peckensis* (Mosasauridae, Plioplatecarpinae), with functional implications for locomotor behavior. *Anat. Rec.* 298, 1597–1611.
 37. David, R., Droulez, J., Allain, R., Berthoz, A., Janvier, P., and Bennequin, D. (2010). Motion from the past. A new method to infer vestibular capacities of extinct species. *C. R. Palevol* 9, 397–410.
 38. Walsh, S.A., Luo, Z.-X., and Barrett, P.M. (2014). Modern imaging techniques as a window to prehistoric auditory worlds. In *Insights from Comparative Hearing Research*. Springer Handbook of Auditory Research 49, C. Köppl, G.A. Manley, A.N. Popper and R. Fay, eds. (London: Springer), pp. 227–261.
 39. Alloing-Séguier, L., Sánchez-Villagra, M.R., Lee, M.S.Y., and Lebrun, R. (2013). The bony labyrinth in diprotodontian marsupial mammals: diversity in extant and extinct forms and relationships with size and phylogeny. *J. Mamm. Evol.* 20, 191–198.
 40. Grohé, C., Tseng, Z.J., Lebrun, R., Boistel, R., and Flynn, J.J. (2016). Bony labyrinth shape variation in extant Carnivora: a case study of Musteloidea. *Journal of Anatomy* 228, 366–383.

41. Benson, R.B.J., Starmer-Jones, E., Close, R.A., and Walsh, S.A. (in press). Comparative analysis of vestibular ecomorphology in birds. *J. Anat.*
42. Grafen, A. (1989). The phylogenetic regression. *Phil. Trans. R. Soc. Lond. B* 326, 119–157.
43. Garland, J.T., and Ives, A.R. (2000). Using the Past to Predict the Present: Confidence Intervals for Regression Equations in Phylogenetic Comparative Methods. *Am. Nat.* 155, 346–364.
44. Soul, L.C., and Benson, R.B.J. (2017). Developmental mechanisms of macroevolutionary change in the tetrapod axis: A case study of Sauropterygia. *Evolution* 71, 1164–1177.
45. Klein, N., Neenan, J.M., Scheyer, T.M., and Griebeler, E.M. (2015). Growth patterns and life history strategies in Placodontia (Diapsida: Sauropterygia). *Royal Soc. Open Sci.* 2: 140440.
46. Pinheiro, J., Bates, D., DebRoy, S., Sarkar, D., and Team, R.C. (2017). nlme: linear and nonlinear mixed effects models. <https://CRAN.R-project.org/package=nlme>.
47. Paradis, E., Claude, J., and Strimmer, K. (2004). APE: analyses of phylogenetics and evolution in R language. *Bioinformatics* 20, 289–290.
48. R Development Core Team (2008). R: a language and environment for statistical computing. R Foundation for Statistical Computing, Vienna, Austria (2008). <http://www.R-project.org>.
49. Pagel, M. (1999). Inferring the historical patterns of biological evolution. *Nature* 401, 877.
50. Bookstein, F.L. (1997). Landmark methods for forms without landmarks: morphometrics of group differences in outline shape. *Med. Image Anal.* 1, 225–243.

51. Gunz, P., Mitteroecker, P., and Bookstein, F.L. (2005). Semilandmarks in Three Dimensions. In *Modern Morphometrics in Physical Anthropology*, D.E. Slice, ed. (Boston, MA: Springer US), pp. 73–98.
52. Gunz, P., and Mitteroecker, P. (2013). Semilandmarks: a method for quantifying curves and surfaces. *Hystrix* 24, 103–109.
53. Wiley, D.F., Amenta, N., Alcantara, D.A., Ghosh, D., Kil, Y.J., Delson, E., Harcourt-Smith, W., Rohlf, F.J., John, K.S., and Hamann, B. (2005). Evolutionary morphing. In VIS 05. IEEE Visualization, 2005., pp. 431–438.
54. Adams, D.C., and Otárola-Castillo, E. (2013). geomorph: an r package for the collection and analysis of geometric morphometric shape data. *Methods Ecol. Evol.* 4, 393–399.
55. Zelditch, M.L., Swiderski, D.L., Sheets, H.D., and Fink, W.L. (2004). *Geometric morphometrics for biologists: a primer*, (Amsterdam: Elsevier Academic Press).

FIGURE LEGENDS

Figure 1. Simplified, time-calibrated sauropterygian phylogeny showing labyrinth shape and relative size change with increasingly pelagic lifestyles (scale of aquatic adaptation further refined in Figure S1). Right labyrinths shown. Red stars indicate labyrinth size reduction events. **A**, *Placodus*; **B**, *Simosaurus*; **C**, *Nothosaurus*; **D**, *Augustasaurus*; **E**, *Macroplata* (left labyrinth reflected); **F**, *Peloneustes* (left labyrinth reflected); **G**, *Microcleidus*; **H**, *Picrocleidus* (dark region placed from disarticulated prootic); **I**, *Callawayasaurus* (left labyrinth reflected. Dark region from opposite prootic of paratype); **J**, *Libonectes*. Labyrinth models not to scale. See also Figures S1–S3 and Table S1. [planned for page width]

Figure 2. Morphospace plots resulting from the principal component analyses. Labyrinth diagrams correspond to anatomical extremes at either end of each PC in lateral and dorsal views. **A**, PC1 vs. PC2. **B**, PC1 vs. PC3. See also Figures S2 and S4, and Tables S1 and S2. [planned for page width]

Figure 3. Sauropterygian labyrinth anteroposterior length plotted against skull (basicranial) length. The bottom-walking placodonts have the relatively largest labyrinths compared to swimming taxa, which generally show an isometric relationship (red line). Short-necked pliosauromorph plesiosaurs have reduced labyrinths. Legend corresponds to Figure 2. See also Figures S2 and S3, and Tables S1 and S3. [planned for column width]

Figure 4. Simplified phylogeny demonstrating right labyrinth shape in various aquatic mammals and reptiles. Colour scheme corresponds to Figure 1 and Figure S1. † denotes extinct taxa. **A**, *Trichechus manatus* (modified and reflected; from [30]). **B**, *Eumetopias jubatus* (reflected; from [30]); **C**, *Tursiops truncatus* (reflected; from [7]); **D**, *Parasuchus angustifrons* (from [25]); **E**, *Pelagosaurus typus* (reflected; from [26]); **F**, *Crocodylus acutus* (reflected; from [27]); **G**, *Aptenodytes forsteri* (from [34]); **H**, *Macrochelys temminckii* (reflected; FMNH 22111); **I**, *Puppigerus camperi* (reflected; NHMUK R 38955); **J**, *Lepidochelys olivacea* (reflected; SMNS 11070); **K**, *Laticauda colubrina* (from [35]); **L**, *Plioplatecarpus peckensis* (from [36]); **M**, *Amblyrhynchus cristatus* (OUMNH 11616); **N**, *Placodus gigas*; **O**, *Simosaurus gaillardoti*; **P**, *Microcleidus homalospondylus*. See also Figures S1–S3 and Table S1. [planned for page width]

STAR METHODS

Contact for Reagent and Resource Sharing

Further information and requests for resources and reagents should be directed to and will be fulfilled by the Lead Contact, James Neenan (james.m.neenan@gmail.com).

Experimental Model and Subject Details

Sauropterygia. The main experimental models are the fossilised crania or partial crania of 19 species of sauropterygian marine reptiles that span their evolutionary history across the Triassic, Jurassic and Cretaceous (Table S1). Adult specimens were selected for this study. Specimen sex is unknown.

Other taxa. For comparative purposes, endosseous labyrinth models were included from four non-sauropterygians and are featured in Figure 4. These are the extant turtles *Macrochelys temminckii* (alligator snapping turtle, FMNH 22111) and *Lepidochelys olivacea* (olive ridley sea turtle, SMNS 11070), the extinct Eocene turtle, *Puppigerus camperi* (NHMUK R 38955), and the extant squamate *Amblyrhynchus cristatus* (marine iguana, OUMNH 11616). Adult specimens were selected and sex is unknown.

Method Details

Dataset assembly. Fossilised cranial material was scanned using either computed axial tomography (CAT; *Edgarosaurus* and *Libonectes*), micro-computed tomography (μ CT; most other taxa), or propagation phase-contrast synchrotron radiation microtomography (PPC-SR μ CT; *Nothosaurus*) (Table S1). Endosseous labyrinths were reconstructed using manual segmentation in Mimics 18.0 and 19.0 (Materialise) for both fully-articulated and partly-disarticulated otic capsules. Our observations suggest that otic capsules disarticulate when subjected to taphonomic compression, and do not undergo plastic deformation that

could alter the geometry of the endosseous labyrinth itself. All specimens (with the exception of *Muraenosaurus*, NHMUK PVR2861) were sufficiently complete to permit measurement of the anteroposterior length of the endosseous labyrinth, and a measurement, or estimate, of the basicranial length of the skull (measured from the anterior surface of the premaxilla to posterior margin of basioccipital condyle; Table S1).

The membranous labyrinth is not preserved in fossils, so here we use the digital endocast of the osseous labyrinth (= endosseous labyrinth) as a proxy for our analyses. Many important and useful features are preserved in the osseous labyrinth, including canal lengths, courses and curvatures, as well as the angles between them (e.g. [37]). These features have been shown to be useful in comparative studies [29, 38-41].

Institutional abbreviations. FMNH, Field Museum of Natural History, Chicago, USA; GPIT, Geological-Palaeontological Institute Tübingen, Germany; LEICT, New Walk Museum and Art Gallery, Leicester, UK; MANCH, The Manchester Museum, UK; NHMUK, Natural History Museum, London, UK; NME, Naturkundemuseum Erfurt, Germany; SAM, South African Museum, Cape Town, South Africa; ROM, Royal Ontario Museum, Toronto, Canada; SMNS, State Museum of Natural History, Stuttgart, Germany; SMUSMP, Southern Methodist University, Shuler Museum of Paleontology, Dallas, USA; TMP, Royal Tyrrell Museum of Palaeontology, Drumheller, Canada; UCMP, University of California Museum of Paleontology, Berkeley, USA; UMO, Urwelt-Museum Oberfranken, Bayreuth, Germany.

Quantification and Statistical Analysis

Scaling relationships for labyrinth size. Labyrinth size scales positively with head mass in tetrapods [12]. Other factors such as agility [8, 41], adaptation to aquatic life [7, 22, 30], and other aspects of locomotory mode [13] modify this scaling relationship. Head size is the most appropriate comparative measure of size, because sensory inputs from the labyrinth

are specifically involved in head stabilisation [12, 13]. We quantified labyrinth size as the anteroposterior length from the base of the anterior canal to the base of the posterior canal because this could easily be measured in 18 of our scans, even when resolution or contrast were insufficient to quantify labyrinth geometry (see below). We tested hypotheses concerning the scaling relationships of the sauropterygian labyrinth using Akaike's information criterion (AICc) to compare phylogenetic generalised least squares (pGLS [42, 43]) regression models including different combinations of a continuous variable (\log_{10} head size) and three categorical variables representing: (1) bottom-walking in placodonts contrasted with swimming in other sauropterygians; (2) pelagic habits (indicated by the presence of flippers) in plesiosaurs contrasted with nearshore habits (indicated by the presence of jointed limbs) in other sauropterygians (Figure 1; Figure S1; Tables S2 and S3); and (3) proportionally short necks in placodonts, thalassophonean pliosaurids and polycotylids contrasting to longer necks in other sauropterygians [15, 44] (Table S1). While analysis of bone histology indicates that placodonts may have had a variety of swimming abilities and life histories [6, 45], it is still generally considered that they were predominantly bottom-walking in order to feed on sessile invertebrates on the sea bed [5]. We do, however, acknowledge that there may be some variation in locomotory styles not only among placodonts, but other Triassic sauropterygians too. The distribution of time-scaled sauropterygian phylogenies presented by Soul & Benson [44] was used as the basis of these analyses, which was conducted using the nlme 3.1-131 [46] and ape 4.1 [47] packages in R version 3.3.2 [48]. Preliminary analyses allowing the strength of phylogenetic signal (λ ; [49]) to vary as a free parameter indicated λ values around 1.0 for all regression models. However, estimating a free λ caused frequent convergence errors. Therefore, we set λ to 1.0 (i.e. pGLS assuming Brownian motion) for the analyses presented herein.

Geometric Morphometrics. Of the specimens scanned, nine provided well-resolved visualisations of the endosseous labyrinth (5 plesiosaurs, 4 other sauropterygians). Due to their better preservation across the sample, right labyrinths were selected for this analysis, with the exception of *Callawayasaurus*, *Macroplata* and *Peloneustes*, where left labyrinths were used and reflected. All endosseous labyrinths were complete, with the exception of *Callawayasaurus*, which was a composite that was assembled by combining the opisthotic and supraoccipital canals of the paratype (UCMP V-125328), with the prootic canals of the holotype (UCMP V-38349). We placed two series of semilandmarks [50-52] along each semicircular canal, one around the shortest route along the internal surface of the canal, and one around the longest, external surface of the canal (Figures S1 and S4), using IDAV Landmark software [53]. Models were all assigned a ‘reference plane’ to ensure accurate landmark placement between taxa, similar to the method used by Yi and Norell [35]. This was achieved by assigning a horizontal plane through the centre of the horizontal canal along its entire length. Landmarks were subsampled to 11 (for internal semilandmark loops) or 12 (for external semilandmark curves) equally-spaced points for each set in the `digit.curves()` function of the `geomorph 3.0.3` package [54] in R. Landmark sets on the internal canal surfaces were treated as closed rings, whereas landmark sets on the external surfaces were treated as open-ended. Procrustes superimposition was applied to remove the effects of scale, orientation, and the arbitrary spacing of semilandmarks, followed by principal component analysis (PCA) to produce a set of geometric variables describing deformations of the labyrinths compared to their mean geometry (shape) [55]. We tested the relationship of major shape variations (PC axes) to body size (i.e. allometry) using the regression approach described above, and to clade membership by visualisation of ordinations (Figure 2, Table S2).

KEY RESOURCES TABLE

REAGENT or RESOURCE	SOURCE	IDENTIFIER
Antibodies		
Bacterial and Virus Strains		
Biological Samples		
<i>Placodus gigas</i>	UMO	BT 13
<i>Cyamodus rostratus</i>	UMO	BT 748
<i>Cyamodus kuhnschnyderi</i>	SMNS	15855
<i>Nothosaurus</i> sp.	NME	16/4
<i>Simosaurus gaillardoti</i>	GPIT	RE/09313
<i>Augustasaurus hagdorni</i>	FMNH	PR 1974
<i>Callawayasaurus colombiensis</i>	UCMP	V-38349
<i>Callawayasaurus colombiensis</i>	UCMP	V-125328
<i>Dolichorhynchops</i> sp.	ROM	29010
<i>Edgarosaurus muddi</i>	MOR	751
<i>Hauffiosaurus tomistomimus</i>	MANCH	LL 8004
<i>Leptocleidus capensis</i>	SAM	K5822
<i>Libonectes morgani</i>	SMUSMP	69120
<i>Macroplata tenuiceps</i>	NHMHUK	R5488
<i>Microcleidus homalospondylus</i>	NHMHUK	36184
<i>Microcleidus macropterus</i>	CAMSM	J 35182
<i>Muraenosaurus leedsii</i>	NHMHUK	PVR2861
<i>Nichollssaura borealis</i>	TMP	94.122.01
<i>Peloneustes phillarcus</i>	NHMHUK	R3803
<i>Picrocleidus beloclis</i>	LEICT	G18.1996
<i>Amblyrhynchus cristatus</i>	OUMNH	11616
<i>Lepidochelys olivacea</i>	SMNS	11070
<i>Macrochelys temminckii</i>	FMNH	22111
<i>Puppigerus camperi</i>	NHMHUK	R38955
Chemicals, Peptides, and Recombinant Proteins		
Critical Commercial Assays		

Deposited Data		
Experimental Models: Cell Lines		
Experimental Models: Organisms/Strains		
Oligonucleotides		
Recombinant DNA		
Software and Algorithms		
R Software	www.r-project.org/	N/A
Mimics	Materialise NV	N/A
Other		

Figure 1

[Click here to download Figure Figure 1.tif](#)

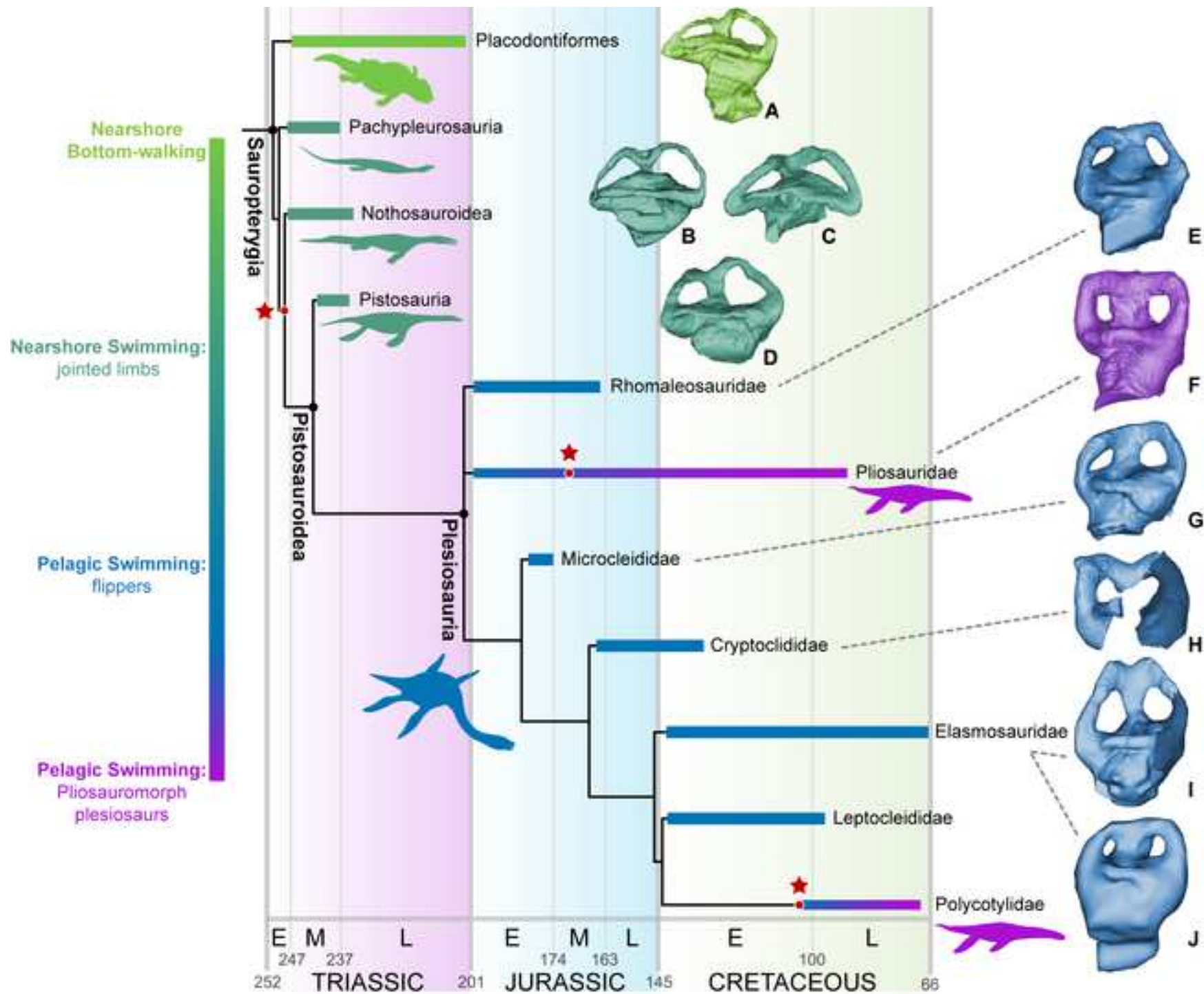


Figure 2

[Click here to download Figure Figure 2.tif](#)

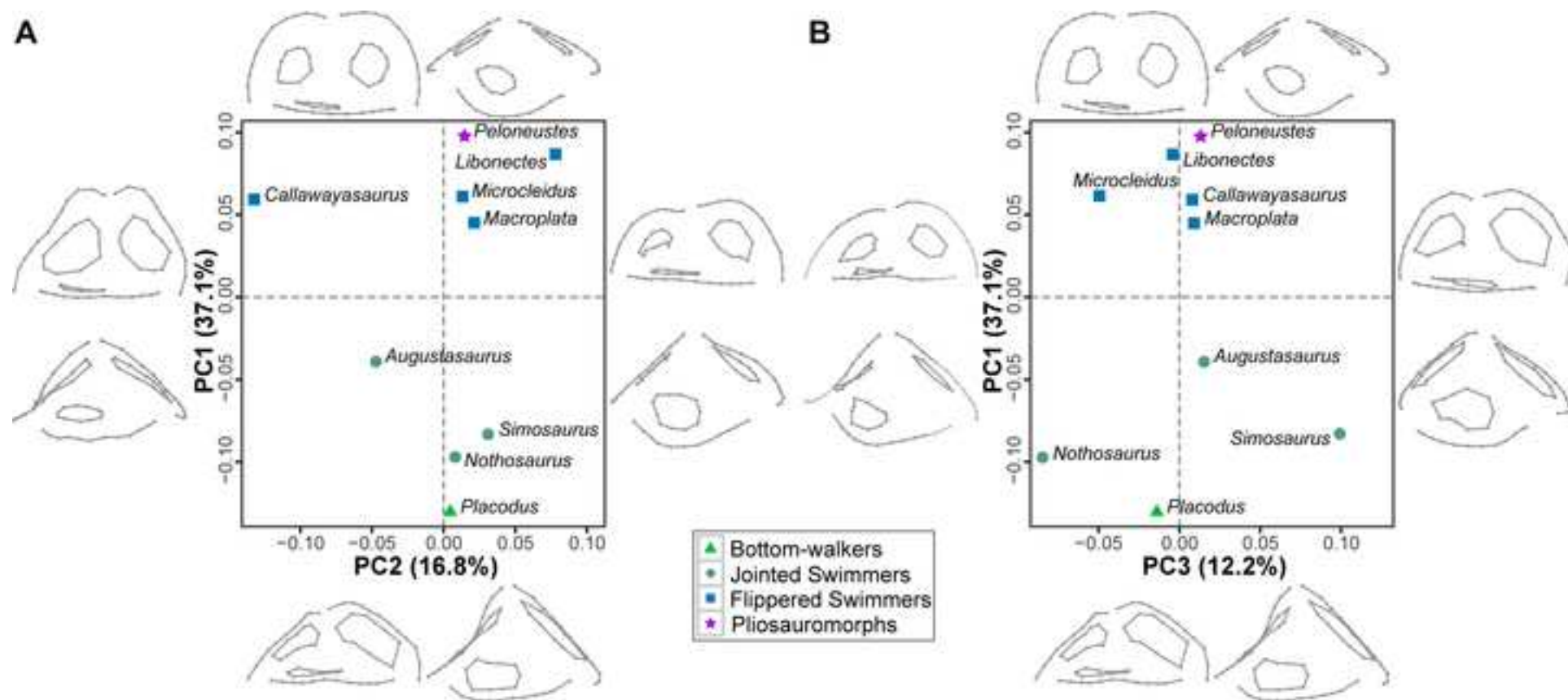
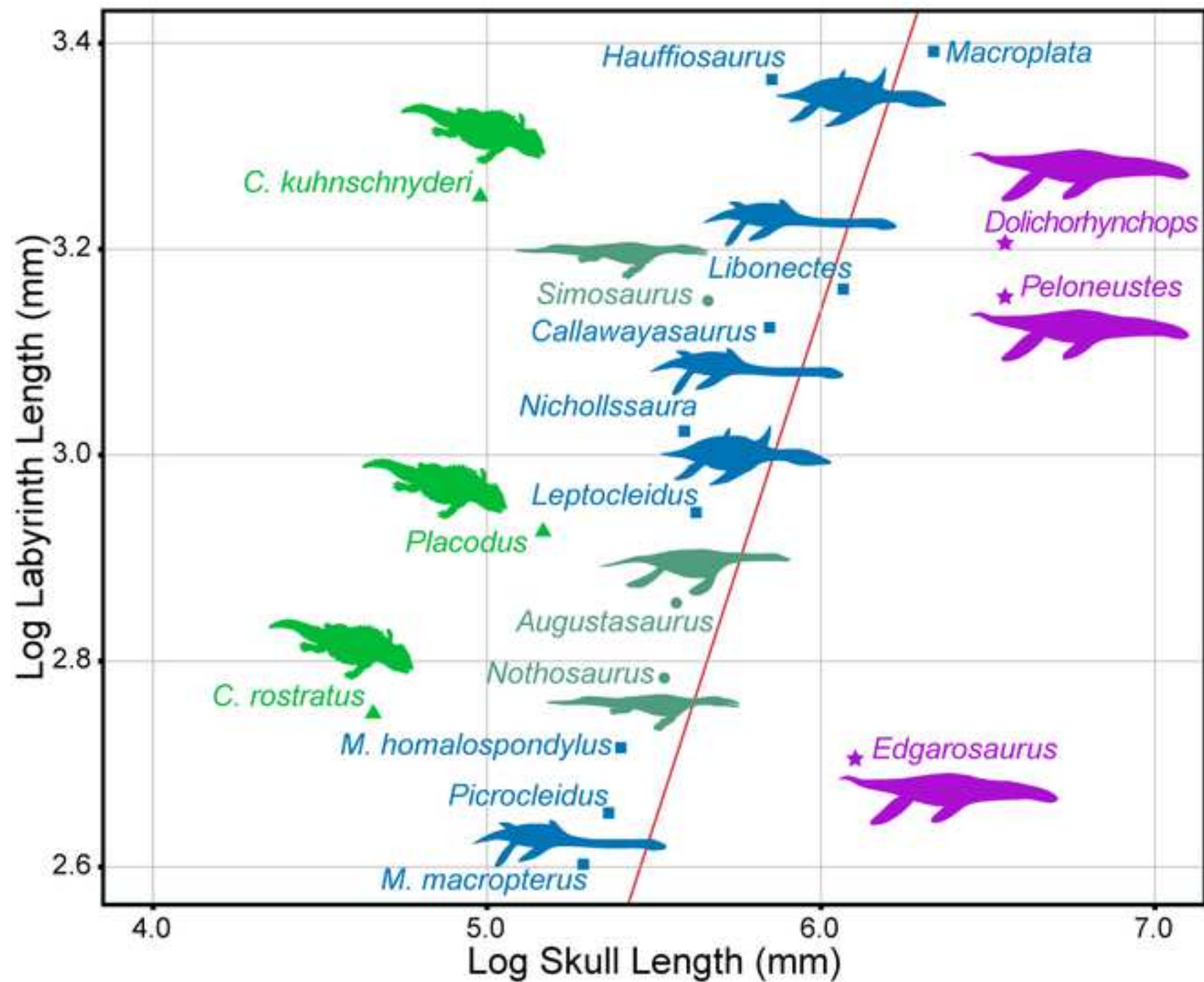
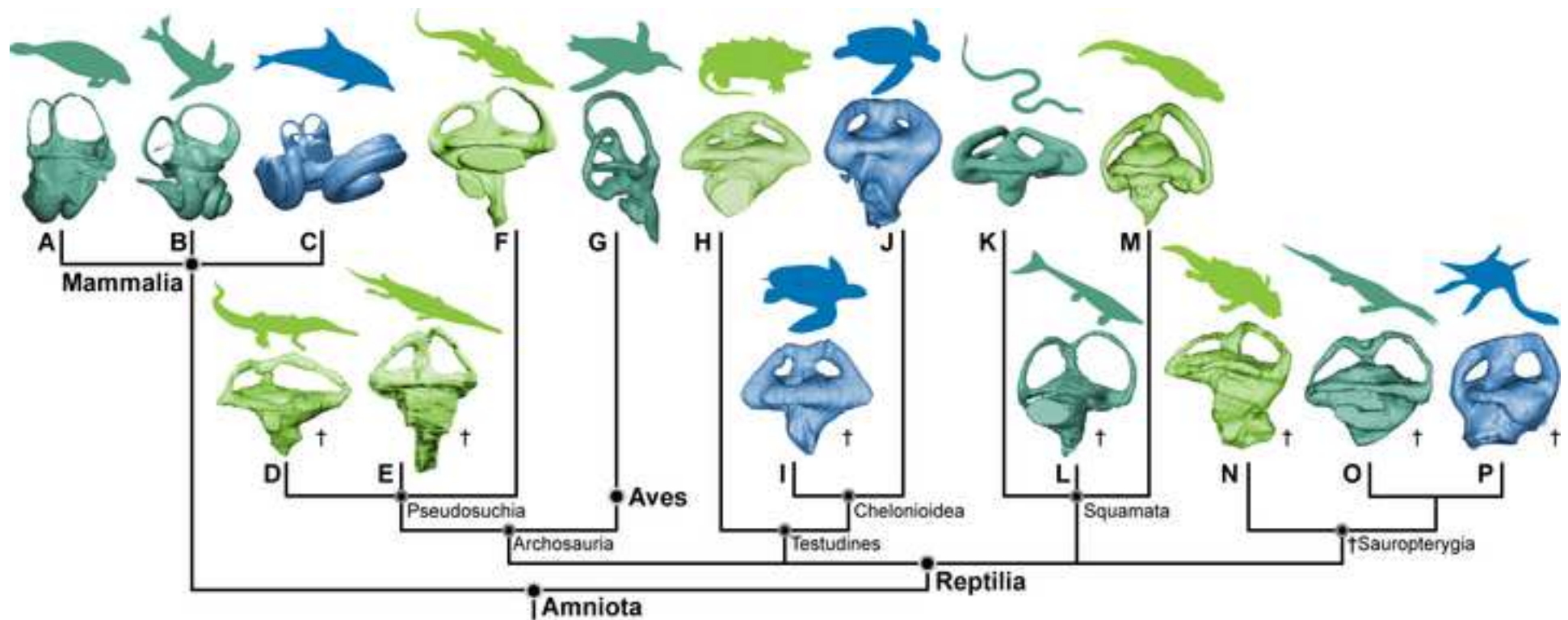


Figure 3

[Click here to download Figure Figure 3.tif](#)



[Click here to download Figure Figure 4.tif](#) 



Nearshore

Terrestrially-adapted,
jointed limbs and bottom-walking



Thalattosauria



Basal sauropterygians



Crocodyliformes

(Teleosauroidae, Pholidosauridae,
Dyrosauridae)



Basal marine squamates

Jointed limbs, often with axial
undulatory locomotion, and
inefficient cruising



Basal ichthyosaurs



Pistosaurs



Metriorhynchoidea



Hydropedal mosasauroids
(Mosasauridae,
Halisauromorpha)



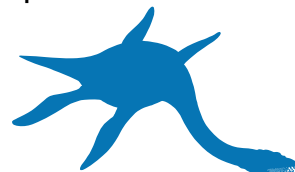
Plotosaurus

Pelagic

Modified limbs (flippers) with a
stiff trunk and efficient cruising



Derived ichthyosaurs
(Parvipelvia + *Californosaurus*)



Derived sauropterygians
(Plesiosauria)



Chelonioidae

Figure S1. Mesozoic aquatic marine reptile evolution (related to Figures 1 and 4). Explanation of the classification system used in this study to denote the degree of aquatic adaptation. Modified from Benson & Butler [S1]. Colour scheme corresponds to Figure 1.

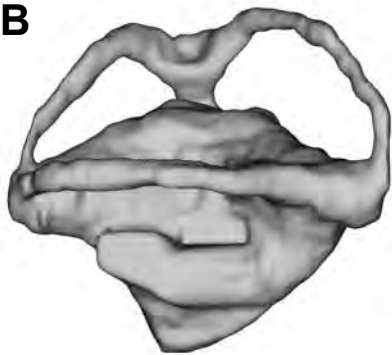
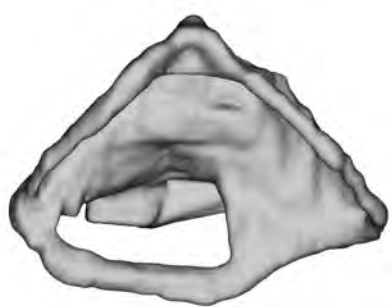
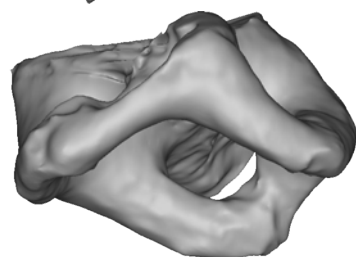
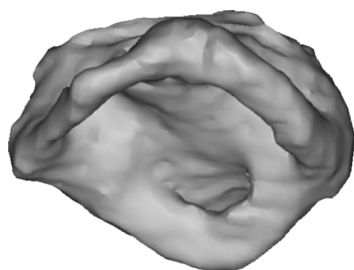
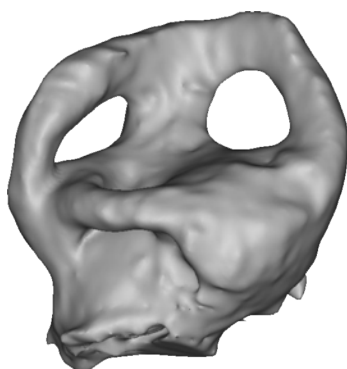
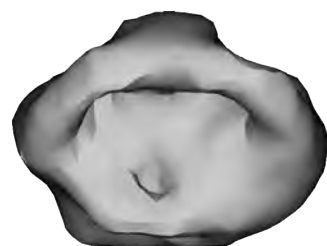
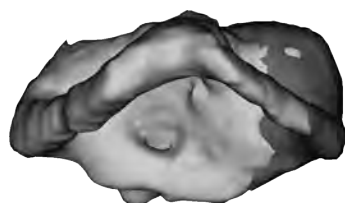
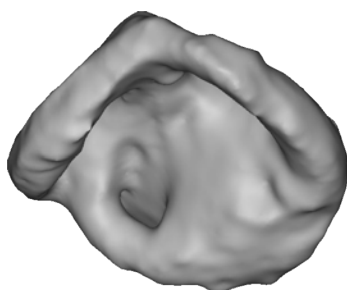
A**B****C****D****E****F****G****H****I**

Figure S2. Right labyrinth models of sauropterygians in lateral (top) and dorsal (bottom) views (related to Figures 1–4). A, *Placodus gigas* (UMO BT 13); B, *Simosaurus gaillardoti* (GPIT/RE/09313); C, *Nothosaurus* sp. (NME 16/4); D, *Augustasaurus hagdorni* (FMNH PR 1974); E, *Macroplata tenuiceps* (reflected; NHMUK R5488); F, *Peloneustes philarcus* (reflected; NHMUK R3803); G, *Microcleidus homalospondylus* (NHMUK 36184); H, *Callawayasaurus colombiensis* (light region reflected from UCMP V-38349, dark region from right prootic of UCMP V-125328). I, *Libonectes morgani* (SMUSMP 69120). Not to scale.

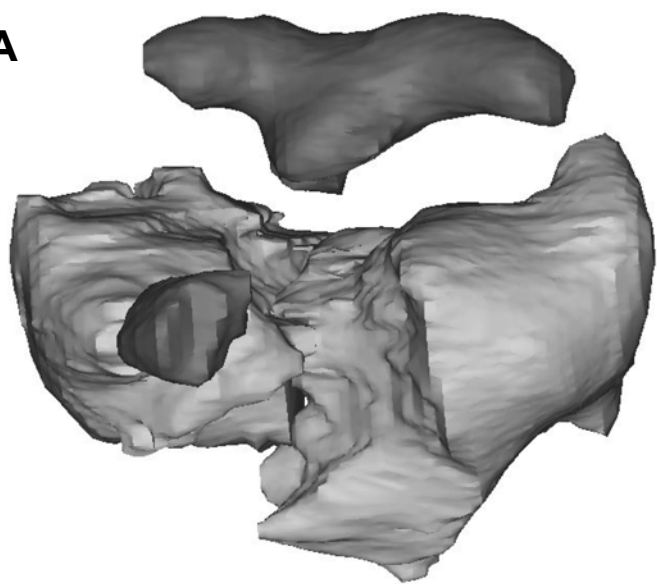
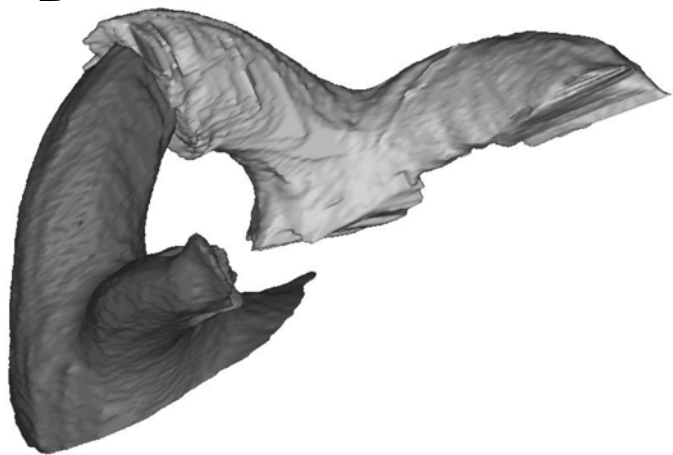
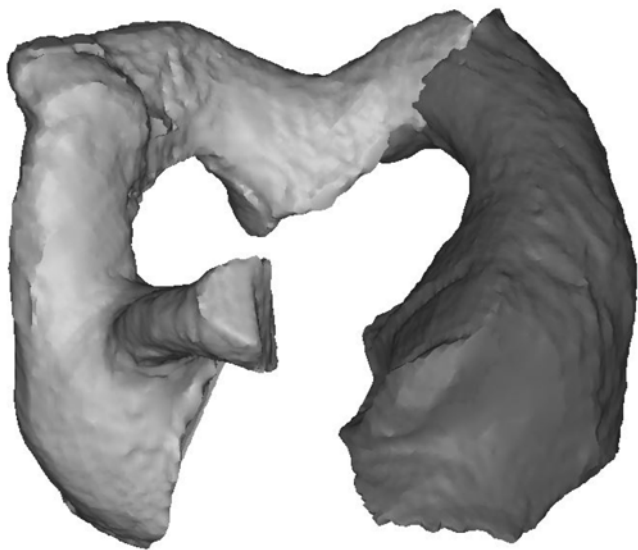
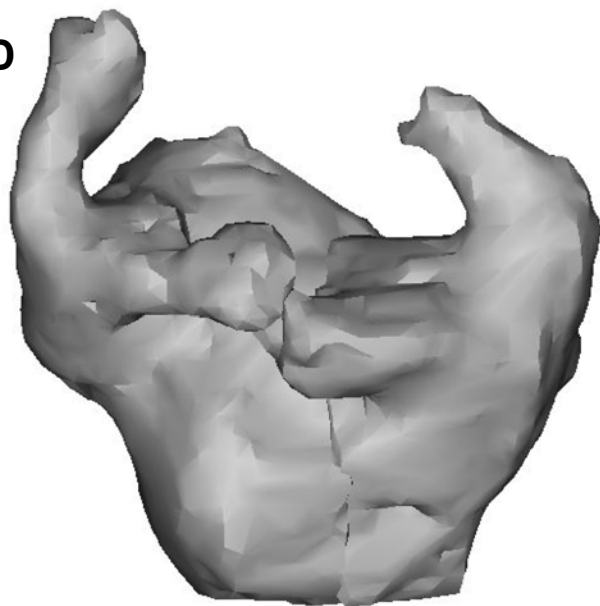
A**B****C****D**

Figure S3. Incomplete right labyrinth models of plesiosaur sauropterygians in lateral view (related to Figures 1, 3 and 4). A, *Hauffiosaurus tomistomimus* (MANCH LL 8004); B, *Muraenosaurus leedsii* (reflected; NHMUK PVR2861); C, *Microcleidus macropterus* (CAMSM J 35182); D, *Nichollssaura borealis* (TMP 94.122.01). Not to scale.

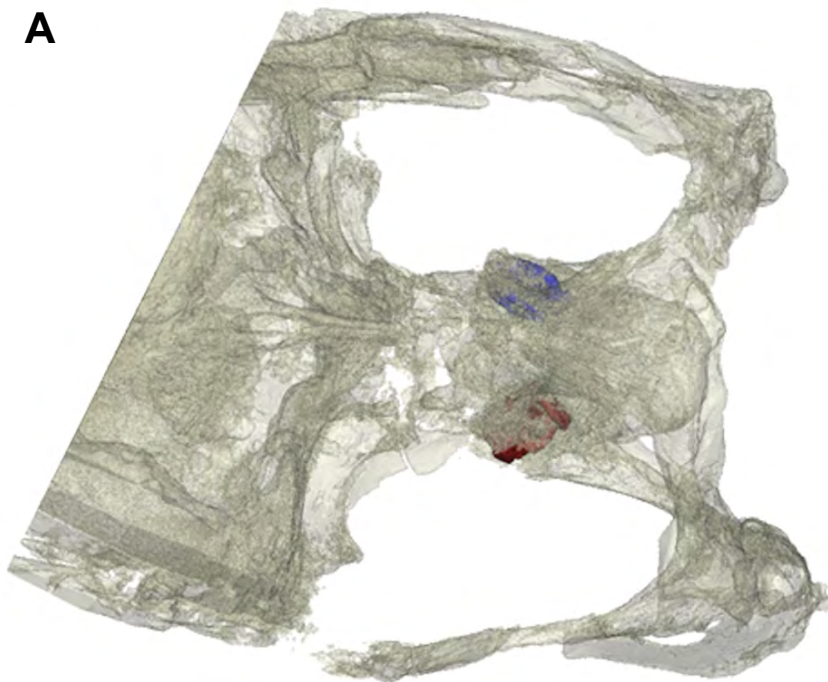
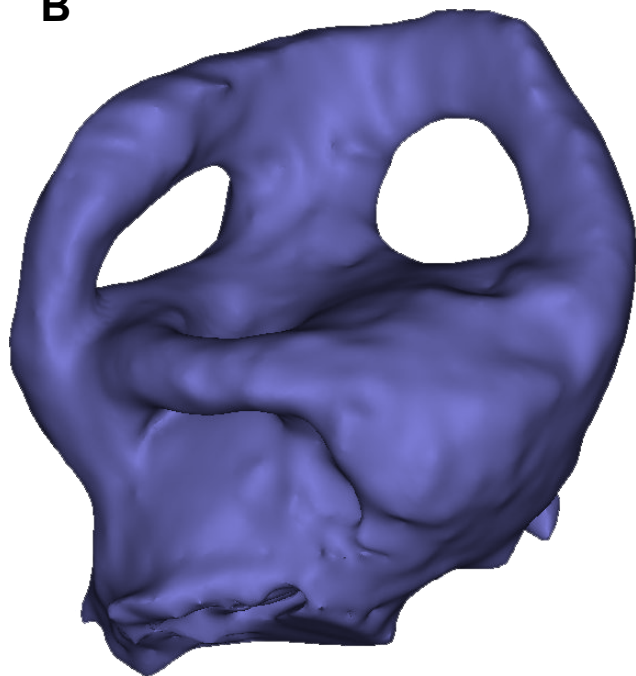
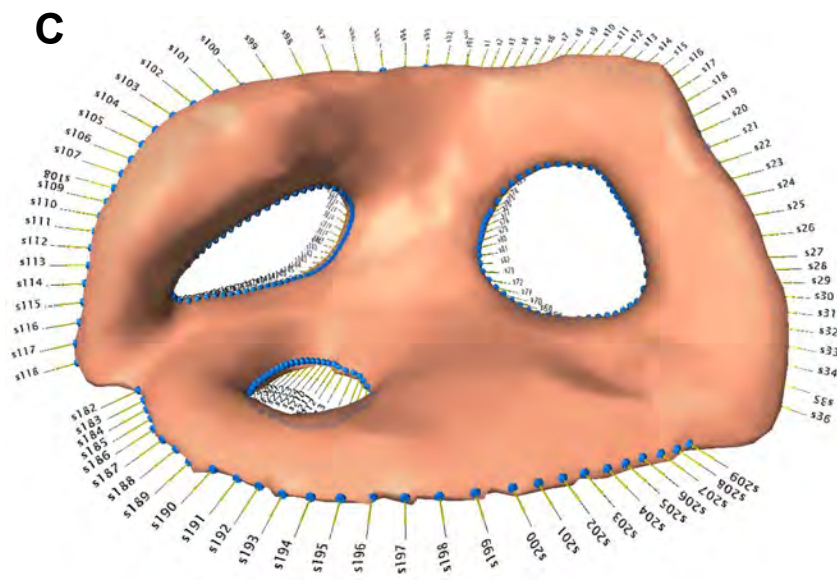
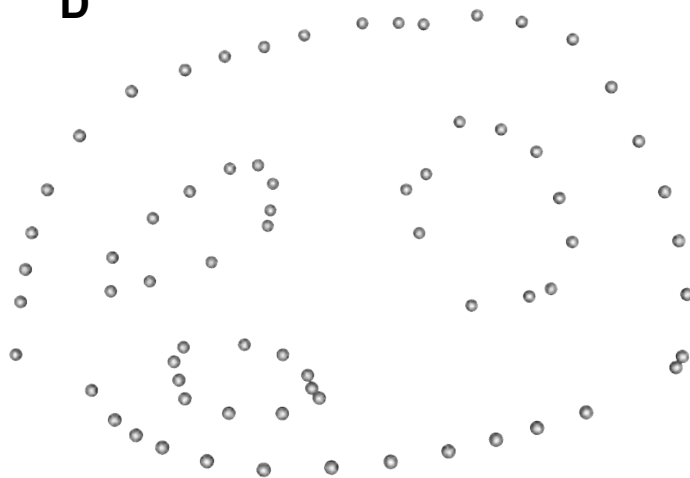
A**B****C****D**

Figure S4. Model creation and landmark placement using *Microcleidus homalospondylus* (NHMUK 36184) as an example (related to Figure 2 and STAR Methods). **A**, labyrinth segmentation within the cranium of NHMUK 36184. The right labyrinth (blue) is selected for analysis. **B**, the fully-segmented right labyrinth. **C**, landmark placement to capture semicircular canal geometry in the software IDAV Landmark [S2]. Note the reference plane which runs through the central axis of the horizontal canal, similar to the method employed by Yi & Norell [S3]. **D**, landmark subsampling to 11 evenly-spaced semilandmarks for internal loops and 12 for external curves using the `digit.curves()` function of geomorph 3.0.3 [S4] in R [S5].

Taxon	Specimen Number	Age	Lifestyle Category	Neck Length	Voxel size (mm)	Basicranial Length	Labyrinth Length	Notes
Placodontia								
<i>Placodus gigas</i>	UMO BT 13	Anisian, M. Triassic	Semi-aquatic_bottom-walking	Short	0.227	175.56	18.65	
<i>Cyamodus rostratus</i>	UMO BT 748	Anisian, M. Triassic	Semi-aquatic_bottom-walking	Short	0.155	105.54	15.63	
<i>Cyamodus kuhnschnyderi</i>	SMNS 15855	Ladinian, M. Triassic	Semi-aquatic_bottom-walking	Short	0.227	145.4	25.82	
Nothosauroidae								
<i>Nothosaurus</i> sp.	NME 16/4	Anisian, M. Triassic	Semi-aquatic_swimming	Intermediate	0.046	247.50	16.3	
<i>Simosaurus gaillardoti</i>	GPIT/RE/09313	Ladinian, M. Triassic	Semi-aquatic_swimming	Short	0.123	304.82	23.3	
Pistosauria								
<i>Augustasaurus hagdorni</i>	FMNH PR 1974	Anisian, M. Triassic	Semi-aquatic_swimming	Intermediate	0.122	261.63	17.4	
Plesiosauria								
<i>Callawayasaurus colombiensis</i>	UCMP V-38349	Aptian, E. Cretaceous	Aquatic_pelagic	Long	0.219	351.90	22.9	Basicranial length taken from holotype specimen (UCMP V-38349). Labyrinth length from a reconstruction from the holotype and paratype (UCMP V-125328).
<i>Callawayasaurus colombiensis</i>	UCMP V-125328	Aptian, E. Cretaceous	Aquatic_pelagic	Long	0.209	-	-	
<i>Dolichorhynchops</i> sp.	ROM 29010	Santonian/Campanian, L. Cretaceous	Aquatic_pelagic	Short	0.154	700.00	24.5	Basicranial length taken from an estimate in Sato et al. 2011 [S6]
<i>Edgarosaurus muddi</i>	MOR 751	Albian, E. Cretaceous	Aquatic_pelagic	Short	0.587	446.87	14.96	
<i>Hauffiosaurus tomistomimus</i>	MANCH LL 8004	Toarcian, E. Jurassic	Aquatic_pelagic	Intermediate	0.066	348.33	28.93	Basicranial length taken from Benson et al. 2011 [S7]
<i>Leptocleidus capensis</i>	SAM-K5822	Valanginian, E. Cretaceous	Aquatic_pelagic	Intermediate	0.158	280.00	19	Basicranial length taken from Cruickshank 1997 [S8]
<i>Libonectes morgani</i>	SMUSMP 69120	Turonian, L. Cretaceous	Aquatic_pelagic	Long	0.742	431.19	23.6	
<i>Macroplata tenuiceps</i>	NHMMUK R5488	Hettangian, E. Jurassic	Aquatic_pelagic	Intermediate	0.320	565.18	29.73	
<i>Microcleidus homalospondylus</i>	NHMMUK 36184	Toarcian, Early Jurassic	Aquatic_pelagic	Long	0.096	221.60	15.12	
<i>Microcleidus macropterus</i>	CAMSM J 35182	Toarcian, Early Jurassic	Aquatic_pelagic	Long	0.083	197.96	13.5	
<i>Muraenosaurus leedsii</i>	NHMMUK PVR2861	Callovian, M. Jurassic	Aquatic_pelagic	Intermediate	0.065	-	-	
<i>Nichollssaura borealis</i>	TMP 94.122.01	Albian, E. Cretaceous	Aquatic_pelagic	Intermediate	0.480	267.95	20.56	
<i>Peloneustes philarcus</i>	NHMMUK R3803	Callovian, M. Jurassic	Aquatic_pelagic	Short	0.093	700.00	23.43	Basicranial length estimated from other specimens.
<i>Picrocleidus beloclis</i>	LEICT G18.1996	Callovian, M. Jurassic	Aquatic_pelagic	Intermediate	0.039	213.60	14.19	Skull not preserved. Length value estimated from anterior tip of dentary to articular condyle.

Table S1. Detailed sauropterygian specimen information (related to Figures 1–4 and STAR Methods).

Model	Type	AICc	N	R ²	Slope	p-value	Intercept	p-value
PC1 ~ centroid size	OLS	-2.72	9	-0.45	0.042	0.221	-0.063	0.286
PC1 ~ centroid size	pGLS	-9.21	9	-1.11	0.007	0.577	-0.093	0.005
PC2 ~ centroid size	OLS	-6.69	9	-0.89	-0.004	0.876	0.006	0.894
PC2 ~ centroid size	pGLS	-3.73	9	-1.02	0	0.982	-0.004	0.907
PC3 ~ centroid size	OLS	-12.83	9	-0.27	0.034	0.056	-0.052	0.09
PC3 ~ centroid size	pGLS	-9.74	9	0.34	0.051	0.003	-0.057	0.039
PC4 ~ centroid size	OLS	-10.77	9	-0.69	0.022	0.249	-0.033	0.317
PC4 ~ centroid size	pGLS	-6.7	9	-0.69	0.02	0.195	-0.015	0.599
PC5 ~ centroid size	OLS	-11.87	9	-1.01	-0.007	0.69	0.01	0.732
PC5 ~ centroid size	pGLS	-10.35	9	-1.18	-0.005	0.652	0.001	0.962

Table S2. Ordinary least squares (OLS) and phylogenetic generalised least squares (pGLS) indicate the absence of correlations of principal component axes describing labyrinth shape with centroid size of the labyrinth (related to Figure 2 and STAR Methods). All estimates of the slope of these relationships have non-significant p-values. R^2 is Nagelkerke's [S9] generalised coefficient of determination and exhibits negative values when our regression models are worse than an intercept-only null model.

Model	AICc weight	AICc	R ²	variable	coefficient	p value
(1) log10(labyrinth size) ~ log10(skull length)	0.64	-15.3	0.27	intercept	0.214	0.558
				log10 (skull length)	0.457	0.008*
(2) log10(labyrinth size) ~ log10(skull length) + swimming	0.15	-12.4	0.27	intercept	-0.035	0.9
				log10 (skull length)	0.605	0.002*
				swimming	-0.161	0.098
(3) log10(labyrinth size) ~ log10(skull length) + swimming + short neck	0.08	-11.2	0.37	intercept	-0.206	0.527
				log10 (skull length)	0.804	<0.001*
				swimming	-0.457	0.008*
				short neck	-0.246	0.031*

Table S3. Phylogenetic generalised least squares (pGLS) regression results for labyrinth size (related to Figure 3 and STAR Methods). Median values of AICc, AICc weight, R^2 , coefficients and p values across analyses on 100 timescaled sauropterygian phylogenies from Soul & Benson [S10] are shown here, and variance around these values is low. Only models with non-negligible AICc weight are shown here, although all combinations of explanatory variables were tested. These included continuous (\log_{10} skull length) and categorical variables: presence of swimming ('swimming') as opposed to bottom walking in placodonts, pelagic habits in plesiosaurs as opposed to nearshore habits in non-plesiosaurs, and a 'short neck' in placodonts and pliosauiromorph plesiosaurs (thalassophonean pliosaurids and polycotylids) [S10, S11], as opposed to longer necks in other sauropterygians. R^2 is the generalised R^2 of Nagelkerke [S9]. $N = 18$ for all analyses.

SUPPLEMENTAL REFERENCES

- S1. Benson, R.B.J., and Butler, R.J. (2011). Uncovering the diversification history of marine tetrapods: ecology influences the effect of geological sampling biases. In *Comparing the Geological and Fossil Records: Implications for Biodiversity Studies*. Geological Society, London, Special Publications, 358, 191–208, A.J. McGowan and A.B. Smith, eds.
- S2. Wiley, D.F., Amenta, N., Alcantara, D.A., Ghosh, D., Kil, Y.J., Delson, E., Harcourt-Smith, W., Rohlf, F.J., John, K.S., and Hamann, B. (2005). Evolutionary morphing. In *VIS 05. IEEE Visualization, 2005.*, pp. 431–438.
- S3. Yi, H., and Norell, M.A. (2015). The burrowing origin of modern snakes. *Sci. Adv.* 1, e1500743.
- S4. Adams, D.C., and Otárola-Castillo, E. (2013). geomorph: an r package for the collection and analysis of geometric morphometric shape data. *Methods Ecol. Evol.* 4, 393–399.
- S5. R Development Core Team (2008). R: a language and environment for statistical computing. R Foundation for Statistical Computing, Vienna, Austria (2008). <http://www.R-project.org>.
- S6. Sato, T., Wu, X.-C., Tirabasso, A., and Bloskie, P. (2011). Braincase of a polycotyloid plesiosaur (Reptilia: Sauropterygia) from the Upper Cretaceous of Manitoba, Canada. *J. Vert. Paleontol.* 31, 313–329.
- S7. Benson, R.B.J., Ketchum, H.F., Noè, L.F., and Gómez-Pérez, M. (2011). New information on *Hauffiosaurus* (Reptilia, Plesiosauria) based on a new species from the Alum Shale Member (Lower Toarcian: Lower Jurassic) of Yorkshire, UK. *Palaeontology* 54, 547–571.

- S8. Cruickshank, A.R.I. (1997). A Lower Cretaceous pliosauroid from South Africa. *Ann. S. Afr. Mus.* 105, 207–226.
- S9. Nagelkerke, N.J.D. (1991). A note on a general definition of the coefficient of determination. *Biometrika* 78, 691–692.
- S10. Soul, L.C., and Benson, R.B.J. (2017). Developmental mechanisms of macroevolutionary change in the tetrapod axis: A case study of Sauropterygia. *Evolution* 71, 1164–1177.
- S11. O'Keefe, F.R. (2002). The evolution of plesiosaur and pliosaur morphotypes in the Plesiosauria (Reptilia: Sauropterygia). *Paleobiology* 28, 101–112.